

Highly Linear InP Phase Modulator for High Dynamic Range RF/Photonic Links

Renyuan Wang[†], Ashish Bhardwaj[#], Sasa Ristic[#], Larry Coldren[#], John Bowers[#], Peter Herczfeld^{*} and Yifei Li[†]

[†]University of Massachusetts at Dartmouth, MA 02747, USA

^{*}Drexel University, Philadelphia, PA 19104, USA

[#]The University of California at Santa Barbara, CA 93106, USA

Abstract — The optical phase locked loop (OPLL) photonic integrated circuit (PIC) is a key element for the emerging linear coherent RF-photonic links. One of the main challenges for the OPLL-PIC is the nonlinearity of the Indium Phosphide (InP)-based phase modulator. In this paper, we report the experimental results from a multi-quantum well phase modulator fabricated on an InP substrate that is specially designed for the OPLL-PIC. The phase modulator shows low optical loss and good linearity performance. In particular, at a reverse bias voltage of 5.6 V, its phase IP3 and insertion loss per unit length are $\sim 2.8\pi/\text{mm}$ and 1.2 dB/mm, respectively.

Index Terms —optical phase locked loop, dynamic range, quantum wells, linear phase modulator.

I. INTRODUCTION

Analog fiber-optic links are attractive for Radar front-end applications in which they connect the antennas to a signal processing unit. The conventional IM-DD fiber-optic links have inadequate spurious free dynamic range (SFDR) due to their intrinsic nonlinearity [1-2]. A novel coherent phase modulated (PM) optical link employing an attenuation-counter-propagating (ACP) optical phase locked loop (OPLL) linear phase demodulator has been proposed for solving the problem arising from the limited dynamic range [3-4]. As shown in Fig. 1, the ACP-OPLL contains an ACP-optical phase modulator, a 3 dB coupler and a pair of balanced high power photodiodes. Using feedback, the ACP-OPLL forces the photodiode output to be a scaled replica of the RF signal driving the phase modulator at the transmitter side. This new optical link aims to achieve a spurious free dynamic range (SFDR) nearing 140 dB·Hz^{2/3}, significantly surpassing the present state-of-the-art.

In order to implement a high bandwidth ACP-OPLL, the ACP-OPLL must be implemented as compact photonic integrated circuit (PIC), where its loop propagation delay is kept at a minimum. An appropriate choice for implementing the local phase modulator inside the ACP-OPLL PIC is an $\text{In}_x\text{Ga}_{1-x}\text{As}_y\text{P}_{1-y}$ -based multi-quantum well (MQW) phase modulator that can be monolithically integrated with low-loss waveguides and photodetectors on an Indium Phosphide (InP)-based material platform.

The major disadvantage with using InP phase modulators is their nonlinearity. The linear modulation range of the phase modulator is characterized by its phase IP3 [6,7], which is

defined as the intercept point of the linear phase modulation response and the third order spurious response in its output phase. Although in theory the phase IP3 of the phase modulator scales linearly with the device length, the high optical loss of existing InP-based optical phase modulators sets a practical constraint on the modulator length and consequently limits the phase IP3 in the range of a couple of π [6]. However, to achieve an SFDR over 140 dB·Hz^{2/3}, a phase IP3 of 10π or larger is required for the phase modulator. In this paper, we present a novel InP-based MQW phase modulator design with a deep ridge optical waveguide which shows a very low optical loss and a good phase IP3 value. This MQW phase modulator design enables an ACP local phase modulator with a phase IP3 of 10π and a 4.3 dB optical loss. In the following sections, we first present the design of the InP-based MQW phase modulator, and then report experimental results from the phase modulator.

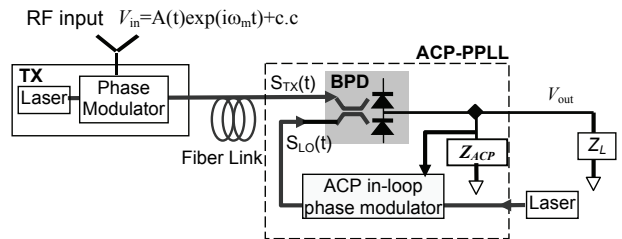


Fig. 1: PM fiber-optic link with ACP-OPLL phase demodulator/detector.

II. INP MQW PHASE MODULATOR DESIGN

InP-based MQW optical phase modulator devices are inherently nonlinear. In order to enhance its linear phase modulation range, the most straightforward approach is to increase the modulator length. This, however, increases the optical propagation loss through the device. For mitigation, we selected a quantum well design [5] where the operating wavelength (~ 1550 nm) is far from the quantum well absorption peak. A schematic of the device cross-section is shown in Fig. 2 along with an SEM image of the device. The phase modulator has a p-i-n diode configuration and is fabricated on a semi-insulating InP substrate. The p-doped layers of the device above the intrinsic MQW region consists of a highly doped ($2 \times 10^{19} \text{ cm}^{-3}$) p-InGaAs contact layer and three subsequent p-InP layers with doping levels of $1 \times 10^{18} \text{ cm}^{-3}$.

3 , $7 \times 10^{17} \text{ cm}^{-3}$ and $5 \times 10^{17} \text{ cm}^{-3}$, respectively from top to bottom. To further reduce the optical loss, a $0.15 \mu\text{m}$ thick undoped InP layer is inserted between the QWs and the p-doped InP to separate the optical mode from the absorptive p-doped InP. Simulation shows that this reduces the optical loss by 0.7 dB/mm . While introducing this undoped InP layer reduces the phase modulation sensitivity, it can be compensated for by increasing the device length. The intrinsic MQW region contains twenty-five periods of 12 nm wide $\text{In}_{0.64}\text{Ga}_{0.36}\text{As}_{0.76}\text{P}_{0.24}$ quantum wells and 8 nm thick InP barriers. The photoluminescence (PL) peak of the QW is at 1370 nm . Below the MQW region is an n-doped InP ($1 \times 10^{18} \text{ cm}^{-3}$) layer followed by a $0.1 \mu\text{m}$ thick n^+ -InGaAsP contact layer. To enhance the optical confinement factor, a deep ridge optical waveguide structure is employed by dry-etching through the MQW region. Then, a mesa structure is formed under the ridge using a selective wet-etch that stops on the $0.1 \mu\text{m}$ thick n^+ -InGaAsP contact layer.

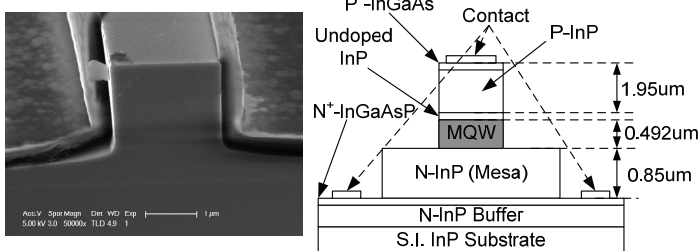


Fig. 2: SEM image and schematic diagram of the cross-section of the InP-based phase modulator.

III. EXPERIMENTAL RESULTS

A. Optical Loss Measurement

The optical loss of the InP MQW phase modulator is measured using an integrated device with two identical 1 mm long phase modulators in series (see Fig. 3). In this measurement, the InP MQW phase modulators are used as photodetectors, where light is launched into one of the phase modulators. Each modulator is reverse-biased at the same voltage, and the photocurrent from each modulator is monitored using two current meters. When the input optical power is sufficiently low, we assume that the photocurrent is proportional to the optical power entering each phase modulator. Since each phase modulator is 1 mm long, the optical loss, α , of the first InP MQW phase modulator is given by:

$$\alpha = 10 \cdot \log_{10} \left(\frac{I_{M1}}{I_{M2}} \right) \quad (1)$$

where I_{M1} and I_{M2} are the photocurrent of the two modulators, and α is expressed in dB/mm . Fig. 4 shows the optical loss versus bias voltage when the wavelength of the input light is 1546 nm and the optical power from the laser source is 6 mW . The optical losses result from the sidewall roughness of the

waveguide and absorption arising in the QWs, free-carrier absorption and the Franz-Keldysh effect. The measured optical loss is very small at low bias voltage ($\sim 0.5 \text{ dB/mm}$). It increases to $\sim 2 \text{ dB/mm}$ as the reverse bias voltage is raised to 6 V .

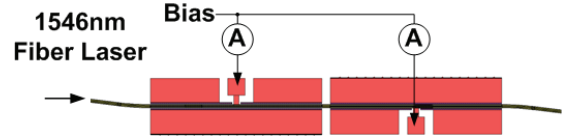


Fig. 3: Experimental setup for measuring the phase modulator loss.

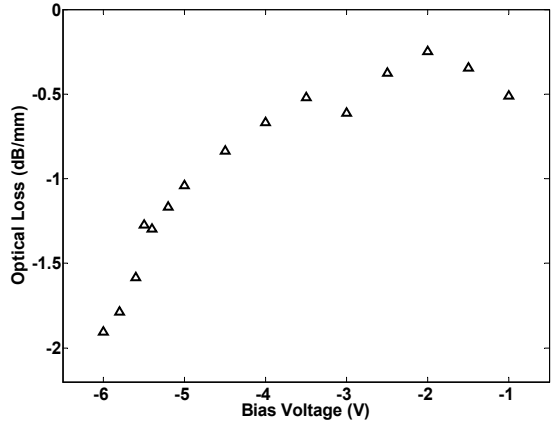


Fig. 4: Insertion loss versus bias voltage.

B. Dynamic V_π Measurement

Since the InP MQW phase modulator has a nonlinear phase modulation response where the PM sensitivity is a nonlinear function of bias voltage. Therefore, the conventional V_π measurement is not suitable to characterize the modulator. In this work, we use dynamic V_π measurement to characterize its PM sensitivity. The dynamic V_π is defined as the ratio between π and the small signal PM sensitivity. The experimental setup is shown in Fig. 5. It consists of a fiber-optic Mach-Zehnder Interferometer (MZI). An InP MQW phase modulator is placed in one arm of the MZI and a commercial LiNbO_3 phase modulator (by EO Space) is placed in the other arm. The small signal PM sensitivity is determined by comparing the InP MQW phase modulator with the known LiNbO_3 phase modulator ($V_\pi \sim 1.2 \text{ V}$). The laser source is a 1546 nm single mode narrow linewidth fiber laser (Orbits Ethernal 2800A-30-PM). A high power erbium doped fiber amplifier (EDFA) (IPG Photonics EAR-3K-C-LP-SF) is used to boost the optical power before it is launched into the MZ interferometer. In the upper arm, the light is coupled to the InP MQW phase modulator waveguide by a tapered fiber with spot size of $2 \mu\text{m}$. The output from the modulator is coupled back into a single mode fiber. The fiber-to-fiber insertion loss is $\sim 12 \text{ dB}$. Thus, a second EDFA is used to amplify the optical power. Three fiber-optic polarization rotators are used in this setup to ensure that light with the correct polarization states are launched into the InP phase

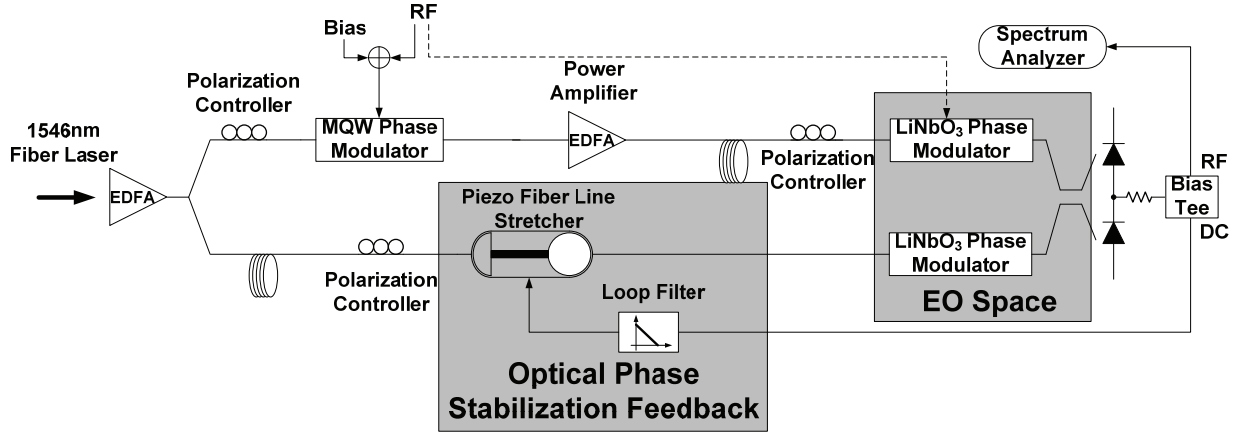


Fig. 5: Experimental setup for dynamic V_π measurement.

modulator, the LiNbO₃ phase modulator and the balanced photodiodes (CC-UTC PD supplied by Photodigm Inc). An HP 8593A spectrum analyzer is used to monitor the RF component of the output from the RF port of the bias tee.

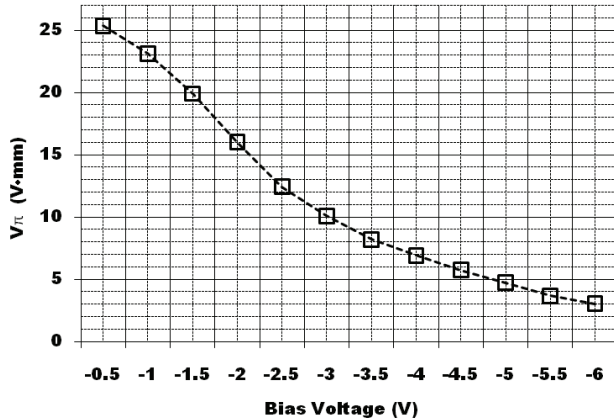


Fig. 6: Dynamic V_π vs. bias voltage.

Because of the temperature fluctuations and mechanical vibrations from the environment, the phase difference between the two interferometer paths suffer from a slow but appreciable drift. Therefore, an optical phase stabilization feedback is implemented. From the DC port of the bias tee, the low frequency spectral components from the output of the photodiodes is extracted and fed into a piezoelectric fiber line stretcher through a loop filter (with a unity gain bandwidth of ~100 Hz). This feedback locks the interferometer at its quadrature point.

To determine the PM sensitivity, a small signal RF tone (11 MHz) is first applied to the LiNbO₃ phase modulator and then applied to the InP MQW phase modulator. For each case, the RF power is monitored at the output of the balanced photodiodes. The RF input power is kept sufficiently low so that the entire interferometer operates in the linear region. The dynamic V_π of the QW modulator is given by:

$$V_\pi^{QW} = V_\pi^{LiNbO_3} \times \sqrt{\frac{P_{out}^{LiNbO_3}}{P_{out}^{QW}}} \quad (2)$$

where V_π^{QW} and $V_\pi^{LiNbO_3}$ are the V_π of the QW modulator and the LiNbO₃ standard, P_{out}^{QW} and $P_{out}^{LiNbO_3}$ are the output RF power from the balanced photodiodes when the same RF input signal is applied to the InP MQW modulator and the LiNbO₃ modulator, respectively. Fig. 6 shows the measured dynamic V_π of the InP MQW phase modulator. The PM sensitivity increases with bias voltage which is consistent with the optical loss measurement, for large absorption change engender large index change according to the Kramers-Kronig relation. When the reverse bias is above 4.7 V, the dynamic V_π is below 5 V for 1 mm long device. With a 3 mm long device, this implies $V_\pi \sim 1.6$ V, which is very efficient when compared to typical LiNbO₃ modulators.

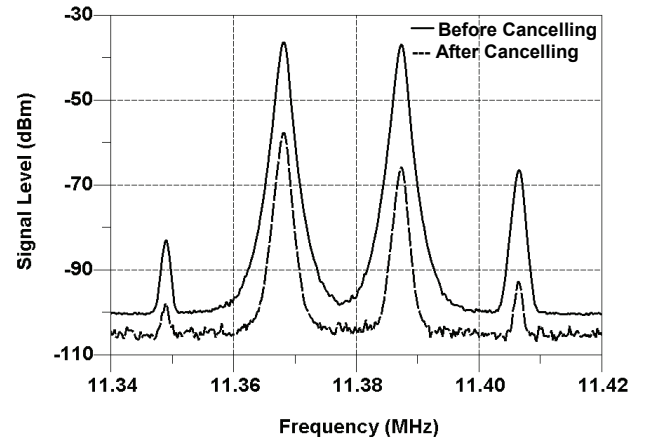


Fig. 7: Spectrum of the MZ interferometer output before and after cancellation.

C. Phase IP3 Measurement

The phase IP3 of the InP MQW phase modulator is determined using the approach reported in [7]. The experimental setup used is similar to that shown in Fig. 5 but with minor modifications. The RF signal is split into two paths using an RF balun (Mini-Circuits ADTL 1-12+). One path is directly applied to the InP MQW modulator placed in one arm of the MZI, while the other is fed to the LiNbO₃ modulator in the other arm of the MZI after passing through a

variable RF attenuator (Mini-Circuits ZX73-2500+). The RF signal contains two tones separated by 20 kHz with a center frequency of 11.38 MHz. By adjusting the attenuation of the signal applied to the LiNbO_3 modulator, we cancel the linear response of the phase modulators. Thus, the third order intermodulation products measured at the output of the balanced photodiodes are solely due to the nonlinearity of the InP MQW phase modulator.

Fig. 7 shows the spectrum of the interferometer output before and after cancelling. The InP MQW modulator is biased at 5.5 V, and the level of the applied two tone signal is -3 dBm at the RF balun.

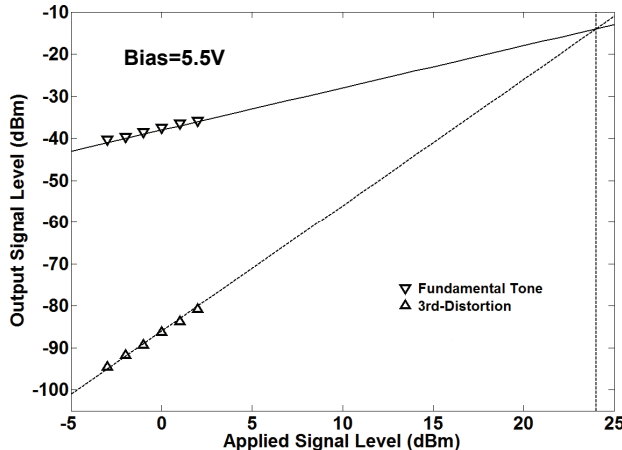


Fig. 8: Input IP3 measurement.

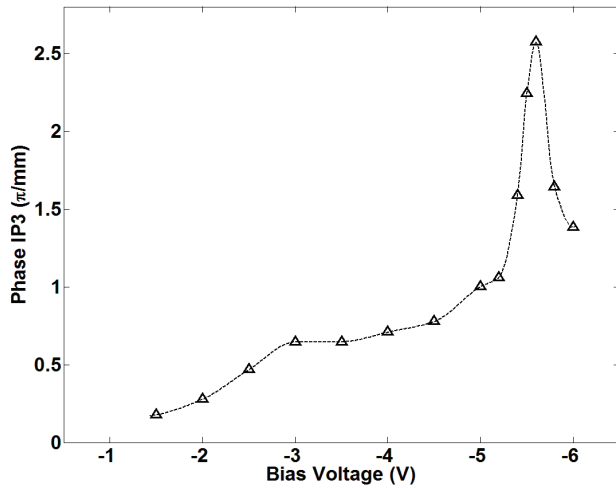


Fig. 9: Measured phase IP3 versus bias voltage.

The linear response of the output is cancelled by more than 20 dB. By applying the same method, the input IP3 of the InP MQW modulator is measured at different reverse bias voltages by sweeping the applied RF signal power. Fig. 8 shows a sample IP3 measurement. The measured Phase IP3 is also plotted as a function of the reverse bias voltage and is shown in Fig. 9. The phase IP3 of the device shows a peak at a reverse bias voltage of 5.6 V. The peak value is $\sim 2.8\pi$ which implies that the phase IP3 of a 3 mm long device is 8.4π . This should support a link with an SFDR nearing $140 \text{ dB}\cdot\text{Hz}^{2/3}$.

The mechanism behind the sharp peak observed in the phase IP3 as a function of reverse bias voltage is still unclear. However, the results are repeatable for the MQW modulators with the same quantum-well design.

IV. CONCLUSION

We have presented the design and experimental studies of an InP-based MQW phase modulator designed for implementing an ACP-OPLL PIC. The measurement shows that the MQW InP phase modulator has a small optical loss and a good phase IP3 value. Specifically, at a reverse bias voltage of 5.6 V its phase IP3 and the optical loss are $2.8\pi/\text{mm}$ and 1.2 dB/mm , respectively. For a 3 mm long device, the modulator design would show a phase IP3 of 8.4π with a tolerable optical loss of 3.6 dB. This is significantly better than the previous reported InP phase modulators [6,7]. This phase IP3 value should enable an RF/photonic link with an SFDR nearing $140 \text{ dB}\cdot\text{Hz}^{2/3}$.

ACKNOWLEDGEMENT

The authors wish to acknowledge Leif Johansson for helping with mounting and wirebonding of the devices and Chad Althouse for valuable suggestions. A portion of this work was done in the UCSB nanofabrication facility, part of the NSF funded NNIN network.

REFERENCES

- [1] E.I. Ackerman, "Broad-band linearization of a Mach-Zehnder electro-optic modulators", *IEEE Trans. Microwave Theory and Tech.*, Vol. 47, pp 2271-2279, Dec. 1999.
- [2] J.H. Schaffner, W.B. Bridges, "Inter-modulation distortion in high dynamic range microwave fiber-optic links with linearized modulators", *IEEE J. of lightwave technology*, vol. 11, pp 3-6, Jan. 1993.
- [3] J. E. Bowers, A. Ramaswamy, L.A. Johansson, J. Klamkin, M.N. Sysak, D.Zibar, L.A. Coldren, M.J. Rodwell, L. Lembo, R. Yoshimitsu, D. Scott, R. Davis, P. Ly, "Linear Coherent Receiver based on a Broadband and Sampling Optical Phase-Locked Loop," *Microwave Photonics '07 (Invited)*, Victoria, Canada, OCTOBER 2007.
- [4] Y. Li, D. Yoo, P. Herczfeld, et al, "Receiver for a Coherent Fiber-Optic Link with High Dynamic Range and Low Noise Figure", Int. Topical Meeting on Microwave Photonics Tech. Dig., pp 273-276, Oct. 2005.
- [5] H. K. Tsang, J. B. D. Soole, H. P. LeBlanc, R. Bhat, M. A. Koza, I. H. White, "Efficient InGaAsP/InP multiple quantum well waveguide optical phase modulator," *Appl. Phys. Lett.* 57, 2285 (1990), DOI: 10.1063/1.103910.
- [6] Y. Li, Renyuan Wang, G. Ding, P. Herczfeld, J. Klamkin, L. Johansson, and J. Bowers, "Novel phase modulator linearity measurement," *Photonics Technology Letters, IEEE*, vol. 21, no. 19, pp. 1405-1407, Oct. 1, 2009.
- [7] M. N. Sysak, L. A. Johansson, J. Klamkin, L. A. Coldren, and J. E. Bowers, "A dynamic measurement technique for third order distortion in optical phase modulators," *IEEE Photon. Technol. Lett.*, vol. 19, no. 3, pp. 170-172, Feb. 1, 2007.